

Analysis of the electronic structure of liquid rubidium by the methods of *ab initio* molecular dynamics, linear muffin-tin orbitals and recursion

This article has been downloaded from IOPscience. Please scroll down to see the full text article.

2008 J. Phys.: Condens. Matter 20 114104

(<http://iopscience.iop.org/0953-8984/20/11/114104>)

View [the table of contents for this issue](#), or go to the [journal homepage](#) for more

Download details:

IP Address: 129.252.86.83

The article was downloaded on 29/05/2010 at 11:07

Please note that [terms and conditions apply](#).

Analysis of the electronic structure of liquid rubidium by the methods of *ab initio* molecular dynamics, linear muffin-tin orbitals and recursion

A A Mirzoev¹, A A Mirzoev Jr², A N Sobolev¹ and B R Gelchinski³

¹ South Ural State University, Prospekt Lenina, 76, Chelyabinsk, 454080, Russia

² Saint-Petersburg State University, Saint-Petersburg, Russia

³ Institute of Metallurgy, Ural Branch of RAS, Yekaterinburg, Russia

E-mail: mirzoev@physics.susu.ac.ru

Received 12 November 2007, in final form 18 January 2008

Published 20 February 2008

Online at stacks.iop.org/JPhysCM/20/114104

Abstract

It is well known that liquid rubidium shows some unusual properties at low densities. The *ab initio* SIESTA package and the supercell technique within the linear muffin-tin orbital method were used to investigate this phenomenon. Electronic structures of liquid rubidium at different temperatures from the melting point up to the critical point were obtained. The atomic structure for the supercell technique was simulated for a cluster of 4000 atoms by the Schommers method on the basis of experimental structure factors of Rb obtained by Tamura and co-workers at different temperatures (from 373 up to 1973 K). The Kubo–Greenwood formula was applied for the calculations of the melt conductivity. The results obtained indicate that the metal–nonmetal transition in liquid rubidium is not connected to the gap at the Fermi energy in the density of electronic states, but, more likely, with electron localization on some kind of atomic cluster.

1. Introduction

Liquid alkaline metals are a convenient object for examinations of the nature and features of density driven metal–dielectric transitions. The cause of this is that the density of alkaline metals changes more than three times on heating from the melting point up to the critical point. Experimental results on the measurement of the electrical conductivity, magnetic susceptibilities, nuclear magnetic resonance (NMR) and neutron diffraction demonstrate unique features of liquid rubidium at densities smaller than 1.0 g cm^{-3} [1, 2] (the rubidium critical temperature, density and pressure are $T_c = 2017 \text{ K}$, $\rho_c = 0.29 \text{ g cm}^{-3}$, $P_c = 124.5 \text{ bar}$ [3]). The data reveal that the precursors of the metal–nonmetal transition play an essential role long before critical point. It is possible to assume that the atomic and electronic structure and dynamics of electrons also change essentially at temperatures long before critical. From the scientific point of view, the main interest is in finding out how the properties of metals vary with large changes in the density. Two points are especially interesting:

the change in the effective interactions of ions immersed in a sea of electrons and the correlation between the behavior of conduction electrons and the disordered state of ions.

The structural changes in thermally expanded liquid rubidium were measured in a pioneering neutron scattering experiment [4] and in high precision synchrotron radiation (SR) diffraction experiments [5]. These experiments indicate that the continuous metal–nonmetal transition is a result of the localization of free conduction electrons at nuclei with ongoing expansion. Although the qualitative explanation is simple, the quantitative theory is very difficult and requires the treatment of many-particle effects in disordered states.

Unfortunately, the theory of structure and electronic properties of liquid metals is still at a primitive stage and the nature of the phase transition at the liquid–vapor critical point has not been well understood. The specified problems are so difficult for the theory of topologically disordered systems that only simulation techniques can provide more insight into changes of physical properties of expanded Rb with density. The most strict and powerful simulation tool now is

ab initio density functional theory based on quantum molecular dynamics (QMD). The first QMD simulations for expanded liquid Rb were carried out in the local density approximation (LDA) [6, 7]. The most extensive study of expanded liquid Rb by the generalized gradient approximation (GGA) method, which suits better inhomogeneous electron density systems near the critical point, was performed by Kietzmann *et al* [8] and Ross *et al* [9]. The detailed analysis of atomic and electronic structure changes in expanded Rb has been carried out carefully in these works, and it has been shown that the metal–nonmetal transition (MNM) occurs smoothly over a wide range of temperatures. This is due to the fact that density decrease is accompanied by such reorganization in atomic structure when there is monotonic decline of the coordination number while the increase of interatomic distances is not so great. In the work [9] the range of Rb density change was divided into three subranges: above 0.5 g cm^{-3} —the metallic state, from 0.5 g cm^{-3} down to 0.3 g cm^{-3} —the region in which clustering takes place, and lower than 0.3 g cm^{-3} —the region of Rb dimer gas.

The restricted number of particles in models is the main deficiency of QMD simulations, that makes the calculation of electrical conductivity and speculations upon the effects of localization impossible. Certainly, this number of particles can be quite enough for the analysis of the atomic and the electronic density of the explored systems. But, if we want to calculate some physical properties for which localization effects are essential (like electrical conductivity or phonon spectra), we can experience difficulties concerning the small size of models. For this reason it is important to use models of maximum size for analyzing properties of expanded alkali metals. Such an opportunity is given by the quasi-*ab initio* LMTO–recursion method that was used by Bose and co-workers (together with the reverse Monte Carlo method (RMC) for constructing the atomic configuration of the system) to calculate the conductivity of liquid and amorphous metals near the melting point (see, e.g., [10, 11]). This method allows us to operate with models of 4–5 thousand atoms. In several works [12, 13] we have improved on the given approach. The first and basic improvement was the generalization of the linear muffin-tin orbital (LMTO) method [14] for low density systems. The computing efficiency of the LMTO method is based on the use of the atomic sphere approximation. The atomic sphere approximation (ASA) is valid if it is possible to divide the space into muffin-tin (MT) spheres centered at various atomic sites. However, the precision of the calculation is determined by the magnitude of the MT sphere overlap and drops strongly with its increase. The latter condition complicates greatly the build-up of MT spheres for systems with loose structure. The presence of pores in atomic structure makes us actually enlarge MT sphere radii, which results in increase of the overlap. Still, it is possible to maintain the feasibility of the ASA approximation by injecting so-called empty spheres (ES), which are MT spheres with smooth potential in loose systems. But, the insertion of empty spheres increases the calculation time; therefore it is essential to find the optimal definition of the ES position, in which the least number of ES fills all volume of the model with overlapping

in certain limits. We suggest using the method of Delaunay simplexes [15] for the search for the optimum ES arrangement. The second modification was exchange of the RMC method for the more precise Schommers method [16]. Our generalization of the LMTO method for the case of low densities requires some additional approximations, such as ES introduction and extrapolation of LMTO Hamiltonian matrix elements to a wide range of interatomic distances. Consequently, it is required to estimate the precision of the method by comparing the results gained by the Schommers–LMTO–recursion (SLR) method with the QMD data. So, the main purpose of our work is to apply the *ab initio* QMD and SLR methods to calculate the properties of liquid rubidium as functions of density over a wide range of temperatures. This will allow us to estimate the applicability of the SLR method for calculating the properties of expanded liquid metals and to explore the nature of changes in conductivity of liquid Rb.

2. QMD and SLR simulations

We have performed *ab initio* molecular dynamics simulations using the Spanish Initiative for Electronic Simulations with Thousands of Atoms code (SIESTA) [17]. SIESTA is both a method and a computer program implementation, designed for performing electronic structure calculations and *ab initio* molecular dynamics simulations of molecules and solids. It uses the standard Kohn–Sham self-consistent density functional method in the LDA or GGA approximation, and norm-conserving pseudopotentials in the fully nonlocal (Kleinman–Bylander) form. Its basis set is a linear combination of atomic orbitals (LCAO) that allows making the computer time and memory scale linearly with the number of atoms, so simulations with several hundred atoms are feasible with modest workstations. We have chosen a simulation box of 128 atoms and periodic boundary conditions; seven valence electrons were considered per atom. The core wavefunctions are modeled using the pseudopotentials (PT) supplied with SIESTA. The particle density in this QMD run was fixed by the total volume of the cubic supercell. Our simulations were performed for a canonical ensemble with the ion temperature regulated by a Nosé–Hoover thermostat.

Another simulation method that we extensively used is the combination of Schommers, LMTO and recursion methods. Initially the atomic structure was simulated for the clusters of 4000 atoms by the Schommers method [16]. Experimental structure factors of Rb obtained by Tamura and co-workers [5] for different temperatures from 373 K ($\rho = 1.5 \text{ g cm}^{-3}$) up to 2123 K ($\rho = 0.59 \text{ g cm}^{-3}$) were used. Then a supercell of 64 atoms for electronic structure calculations was selected from this cluster. Local electronic structure and partial densities of states for separate atoms were found by the LMTO method [14]. At the same time a 64-atom ensemble is quite enough for the precise calculations of the thermodynamic average values and finding the structural characteristics of a system.

We have used the scalar-relativistic version of LMTO in ASA. The local density approximation with the von Barth–Hedin form of the exchange–correlation potential was

used. For the correct description of a disordered expanded system, from 30 up to 60 empty spheres were injected in a cell of 64 Rb atoms. The atomic sphere radii were chosen according to the charge neutrality condition, and were adjusted automatically during iterations toward self-consistency to satisfy this condition. The electronic density of states was calculated by integration on a Brillouin zone with the subsequent smoothing of discrete atomic energy levels. The width of the Gaussian used for smoothing was 0.095 eV. Finally the averaging over all atoms in the cell was performed.

To obtain the conductivity we have used the first-principles tight-binding linear muffin-tin orbitals (TB-LMTO) Hamiltonian [14] in the recursion method [18, 19] to calculate the electron density of states (DOS) and the electron eigenstates for 4000- and 8000-particle liquid rubidium clusters with periodic boundary conditions. Application of the LMTO-recursion method has allowed us to increase the size of the explored system. It has made it possible to study the effect of the localization of electronic states on liquid metal conductance. Although self-consistency in an average sense could be achieved for a small number of atoms, we have relied on the fact that the potential parameters are the true atomic quantities in the Hamiltonian. They are obtained from the solution of the wave equation at the sphere boundary, and hence depend on the volume per atom. We can obtain this dependence from our supercell LMTO-ASA calculations for a 64-atom cluster of liquid Rb with periodic boundary conditions. It might be mentioned that self-consistent potential parameters practically do not depend on the close atomic environment and are well approximated by the formula containing a single parameter—the radius of the MT sphere [14].

According to the Kubo-Greenwood formula, diagonal elements of the conductivity tensor at 0 K can be written in a physically transparent form:

$$\sigma_{jj} = \frac{e^2}{\Omega_a} n(E_F) D(E_F). \quad (1)$$

Here Ω_a is the atomic volume, $n(E_F)$ is the DOS falling on one atom and $D(E_F)$ is the diffusivity function, that can be calculated as follows:

$$D(E_F) = -\hbar \lim_{\epsilon \rightarrow 0} \text{Im} \{ \langle E_m | \hat{v}_j \hat{G}(E_F + i0) \hat{v}_j | E_m \rangle \} |_{E_m=E_F} \quad (2)$$

where $G(E)$ is the Green function of system and v_j is the j th component of the velocity operator, which can be expressed in the TB-LMTO approach through the matrix elements of the TB Hamiltonian and atomic coordinates:

$$\hat{v}_j = \frac{[\hat{H}, \hat{x}_j]}{\hbar}. \quad (3)$$

It is easy to see that $D(E_F)$ can be represented as the average local DOS projected on the states $v_j | E_m \rangle$ and can be calculated using the recursion method. The most time-consuming part is the search for an eigenvector with definite energy. We used the filtration procedure described in [20]. The filtering operator

$$\hat{D} = \frac{(\hat{H} - a)(\hat{H} - b)}{\Delta^2} \quad (4)$$

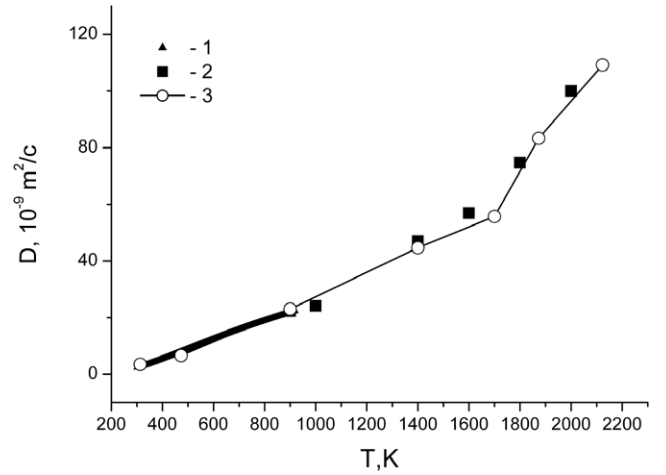


Figure 1. The comparison of the diffusion coefficient calculated by the QMD method with experimental data: 1—data [21]; 2—data extracted from viscosity measurements [22]; 3—our results.

has been used, where $a = E_F - \Delta/2$, $b = E_F + \Delta/2$, Δ is the width of the filtering zone. The parameter Δ changes dynamically during the filtration.

3. Results for pair correlation function and dynamic properties

First, to show the reliability of our QMD simulation we compare the calculated diffusion coefficient with experimental data [21] in figure 1.

In figure 2 we compare the pair correlation functions (PCF) $g(R)$ at 373 and 1873 K calculated by our methods with the experimental results [5]. From figures 1 and 2 one can see that calculated and experimental results are in good agreement, which means that we can rely on our QMD method in reproducing the structure and properties of liquid rubidium for a wide range of temperatures. One cannot speculate on the nature of the MNM transition without information about the structure of the melt. Traditionally the structure of a fluid is understood as the structure of the short-range order, which is defined by the assignment of distance up to the nearest neighbors (R_i) and their average number (N_R), i.e. those parameters which can be found from diffraction experiments. However, determination of these quantities from the diffraction data is carried out by various methods which give either certainly overstated or underestimated values of the indicated parameters.

At the same time, it is necessary to point out that we can rely on these estimations only near to the melting point T_m , where the peak of function $g(R)$ is clearly seen and is symmetrical enough. In the high temperature region, where the function $g(R)$ is essentially smoothed (right part of figure 2), the degree of accuracy of these methods is reduced, and the acceptability of its use requires extra substantiation. For example, the density variations in the coordination number N_i which is derived in [5] by integrating the PCF up to the first-minimum position and in [1] twice up to first-maximum position are different, especially at high temperatures. In this

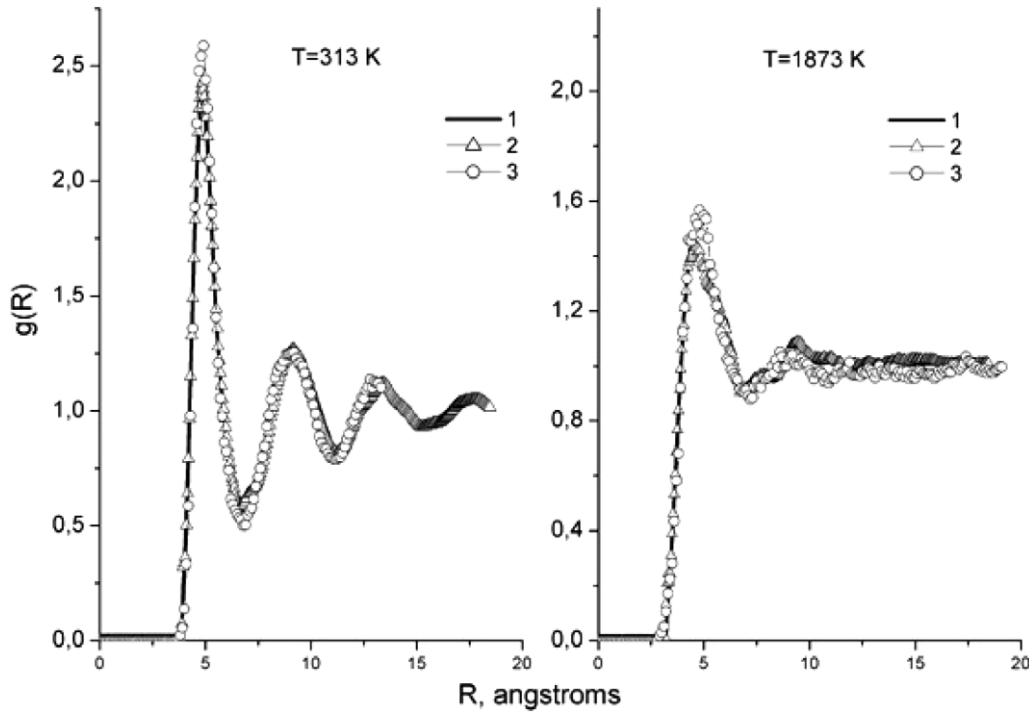


Figure 2. The comparison of the PCF calculation results with experimental data: 1—experimental data [5]; 2—SLR results; 3—QMD results.

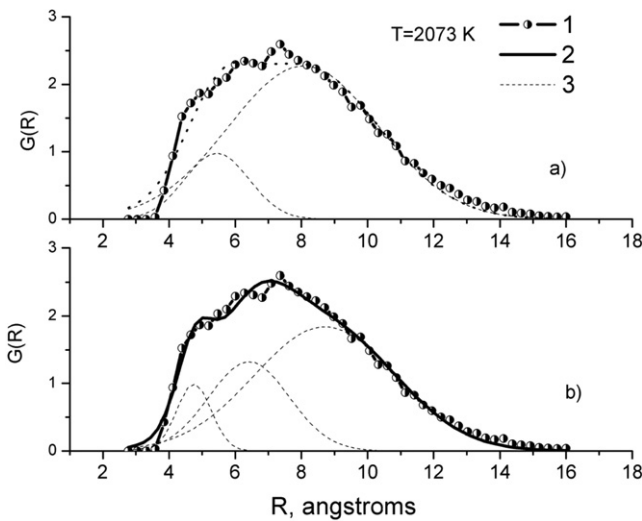


Figure 3. The results of multi-Gaussian analysis of the $G(R)$ distribution at different temperatures.

connection there is a problem of development of adequate (taking into account specific features) and more precise methods while evaluating short-range order structure. We suggest applying the method of Voronoi polyhedra (VP) and Delaunay simplexes (DS) [16] giving unique information about the structure of the short-range order and consequently permitting us to develop more precise measurement for this purpose. The most specific features of the VP method used in the present work are the average number of sides (neighbors) in a Voronoi polyhedron (that corresponds to the number of

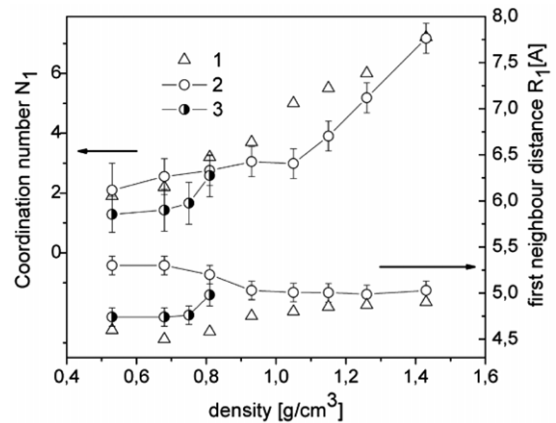


Figure 4. Density variation of coordination numbers and first-neighbor distances: 1—results [8]; 2—our results which are derived by two-Gaussian analysis of $G(R)$; 3—our results which are derived by three-Gaussian analysis of $G(R)$.

geometrical neighbors of an atom) and the distribution of the number of neighbors in the radial distance from the center—the $G(R)$ distribution, which is similar to

$$N_R = 4\pi\rho g(R)R^2\Delta R, \quad (5)$$

which is the number of nearest neighbors in an interval of distances from R up to $R + \Delta R$, but it takes into account only those neighbors which will yield a VP. At small distances, functions N_R and $G(R)$ coincide, and at major R , the function $G(R)$ promptly decreases to zero.

Using $G(R)$ decomposition into Gaussian multi-peaks it is possible to analyze the fine short-range order structure

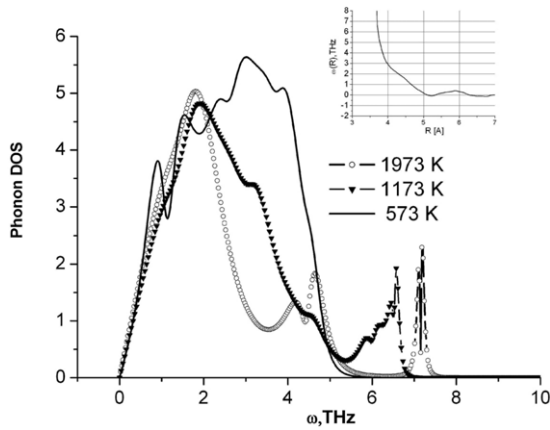


Figure 5. Temperature dependence of the liquid rubidium phonon state density.

of expanded metals. We can see the results of such decompositions on an example of $G(R)$ distribution. The latter can be submitted with good precision as the total of two Gaussians which can be interpreted as contributions of the nearest neighbors and neighbors from the second coordination sphere.

Only for temperatures higher than 1573 K is there an appreciable discrepancy of such representation with the actual

distribution function in the 3–4 Å range of distances. This means the apparent occurrence of additional coordination relating to formation of the molecular clusters of rubidium.

In figure 3 the result of application of that technique to the structure analysis of Cs melt compared with data [8] is shown. Carrying out the dissection of the $G(R)$ distribution not on two but to three peaks, for temperatures higher than 1573 K the standing of the new peak corresponds to distances of 4.2–4.8 Å that coincide with bond lengths of neutral and ionized dimers Rb_2 as shown in [24]. The reliable values of the coordination numbers that we obtained differ from those of [5]. Figure 4 shows that the coordination number decreases substantially and almost linearly with density decrease from 1.5 to 1.1 $g\ cm^{-3}$ and then shows a strong deviation from a linear dependence, equal to approximately 6 until reaching 0.7 $g\ cm^{-3}$, and after that lowering to values corresponds to small molecular Rb clusters. Thus, our calculations essentially change boundaries of areas of rubidium melt density with various types of structure marked out in [9].

In figure 5 we present the result of phonon density of states calculations. The details of the calculation can be found in [25]. It is visible that at low temperatures the phonon spectrum lies in the low frequencies range and is continuous. But at higher temperatures we can see the occurrence of a local mode. In the inset of figure we showed the dependence of the oscillation frequency for two Rb atoms which are interacting

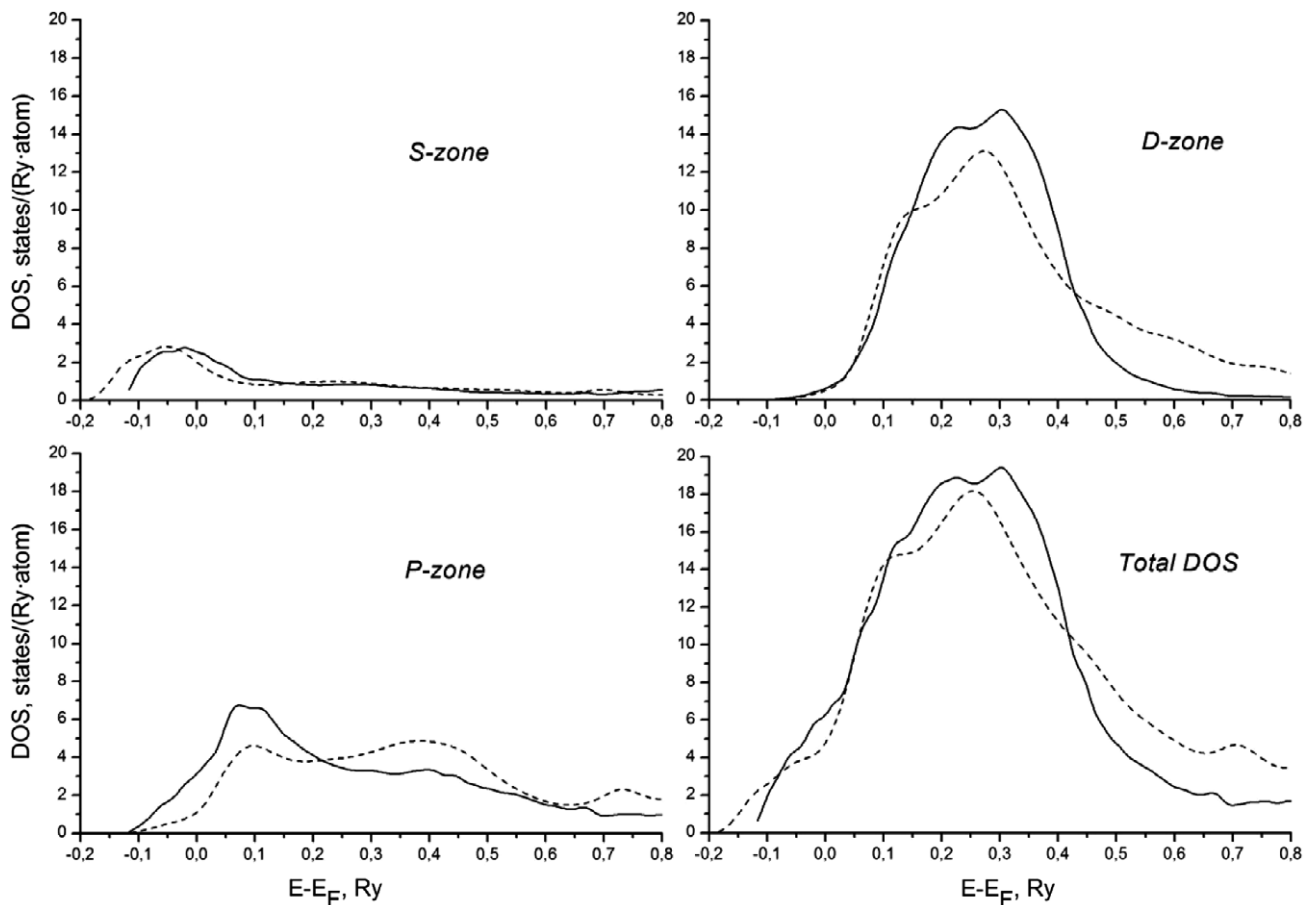


Figure 6. Rb DOS at 1673 K. Solid line—QMD calculations; dotted line—SLR calculations.

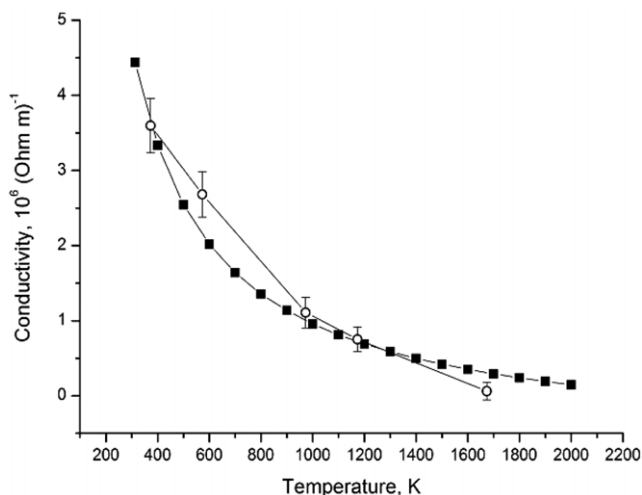


Figure 7. Temperature dependence of changes of the conductivity of liquid rubidium: full squares—experimental data [23]; empty circles—results of our calculation.

by means of the calculated Schommers potential. As we can see from the inset, this mode corresponds to the interatomic distance of about 4 Å which is the length of the bond in the rubidium dimers [24].

4. Electronic properties

Besides the structure dependent properties, electronic properties such as the DOS were obtained from QMD and SLR methods (figure 6).

Evidently, the results show good enough agreement. The DOS at the Fermi energy decreases monotonically with temperature increasing and does not change much. In the electron density distribution in the Rb melt at 1673 K one can see that the electron density becomes strongly inhomogeneous at this temperature. We can see areas of high density localized and directed in space, which interconnect 2–3 atoms. This result is in agreement with data in previous works [10].

The conductivity was calculated using the Kubo–Greenwood formula (1), (2). The results of our calculations are presented in figure 7 and are compared with existing experimental data [23]. The results are fitted to experiment within error limits of 20%. However, the principal feature of the present calculation is the fact that it is free from any fitted parameters. It is obvious from (1) that the conductivity depends on two factors: the first is the DOS at the Fermi level and the second is the diffusion mobility $D(E_F)$ (2). The behavior of the diffusion mobility $D(E_F)$ indicates a sharp reduction of the electron mobility leading to electron localization at higher temperatures.

5. Conclusions

We have performed extensive simulations by QMD and by the combination of Schommers, LMTO and recursion (SLR) methods for expanded fluid Rb. The agreement of the calculated pair correlation functions with experimental

results is good, which means that we can rely on our QMD method for reproducing the structure and properties of liquid rubidium for a wide range of temperatures. The theoretical coordination numbers and next-neighbour distances follow the experimentally determined trends along the expansion. This behavior can be explained within a bond-network problem. The DOS and electronic charge density extracted from the QMD and SLR simulation methods show qualitatively the transition from a metallic to a nonmetallic state with the thermal expansion of the liquid from the melting point to the region of the critical point. The SLR method is not *ab initio* in the strict sense; nevertheless it provides good results on structural and electronic properties of liquid metals over a wide temperature region up to the critical point. In addition this method allows us to obtain large scale models of melts and calculate such properties as conductivity that cannot be obtained using small size models. The nature of the abrupt conductivity decrease in rubidium lies in the appearance of some sorts of clusters such as Rb_2 and Rb_3 , which possibly occurs already at temperatures higher than 1400 K up to the critical point, in agreement with earlier predictions of advanced chemical models and other QMD simulations.

Acknowledgments

This work was financially supported by the Russian Foundation for Basic Research, projects Nos 06-03-32690 and 06-08-01142.

References

- [1] Hensel F and Uchtmann H 1989 *Ann. Rev. Phys. Chem.* **40** 61–83
- [2] Redmer R and Warren W W 1993 *Phys. Rev. B* **48** 14892–906
- [3] Jungst S, Knuth B and Hensel F 1985 *Phys. Rev. Lett.* **55** 2160–3
- [4] Franz G, Freyland W, Glaser W, Hensel F and Schneider E 1980 *J. Physique Coll.* **41** C8
- [5] Matsuda K, Tamura K and Inui M 2007 *Phys. Rev. Lett.* **98** 096401
- [6] Cabral B J C and Martins J L 1995 *Phys. Rev. B* **51** 872–7
- [7] Shimojo F, Zempo Y, Hoshino K and Watabe M 1995 *Phys. Rev. B* **52** 9320–9
- [8] Kietzmann A, Redmer R, Hensel F, Desjarlais M P and Mattsson T R 2006 *J. Phys.: Condens. Matter* **18** 5597–605
- [9] Ross M, Yang L H and Pilgrim W C 2006 *Phys. Rev. B* **74** 212302
- [10] Bose S K, Jepsen O and Andersen O K 1994 *J. Phys.: Condens. Matter* **6** 2145–58
- [11] Skriver H L 1984 *The LMTO Method: Muffin-Tin Orbitals and Electronic Structure* (Berlin: Springer)
- [12] Vorontsov A G and Mirzoev A A 2002 *Melts* **3** 33 (in Russian)
- [13] Vorontsov A et al 2007 *J. Non-Cryst. Solids* **353** 3206–10
- [14] Andersen O K and Jepsen O 1984 *Phys. Rev. Lett.* **53** 2571–4
- [15] Medvedev N N 2000 *Voronoi–Delaunay Method for Non-crystalline Structures* (Novosibirsk: SB RAS) (in Russian)
- [16] Schommers W 1983 *Phys. Rev. A* **28** 3599–605
- [17] Soler J M, Artacho E, Gale J D, Garcia A, Junquera J, Ordejon P and Sanchez-Portal D 2002 *J. Phys.: Condens. Matter* **14** 2745–79
- [18] Haydock R 1980 *Solid State Phys.* **35** 215–94

- [19] Nowak H J, Andersen O K, Fujiwara T, Jepsen O and Vargas P 1991 *Phys. Rev. B* **44** 3577–98
- [20] Kramer B and Weaire D 1978 *J. Phys. C: Solid State Phys.* **11** L5–7
- [21] Ohse R W 1985 *Handbook of Thermodynamic and Transport Properties of Alkali Metals* (Oxford: Blackwell)
- [22] Belaschenko D K 2006 *Russian J. Phys. Chem. A* **80** 1567–77
- [23] Bystrov P I and Kagan D N *et al* 1990 *Liquid Metal Coolants for Heat Pipers and Power Plants* (New York: Hemisphere)
- [24] Krauss M and Stevens W J 1990 *J. Chem. Phys.* **93** 4236
- [25] Vorontsov A, Mirzoev A, Vyatkin G and Sobolev A 2007 *J. Non-Cryst. Solids* **353** 3206